Available online at www.sciencedirect.com
ScienceDirect
Journal of Catalysis 246 (2007) 109–117
JOURNAL OF CATALYSIS
www.elsevier.com/locate/jcat

A density functional theory study of the hydrogenolysis and elimination reactions of C_2H_5SH on the catalytically active (100) edge of 2H-MoS_2

Teodora Todorova, Roel Prins, Thomas Weber *

Institute for Chemical and Bioengineering, Swiss Federal Institute of Technology (ETH), Wolfgang-Pauli-Strasse 10, HCI E 117, CH-8093 Zurich, Switzerland

Received 7 August 2006; revised 15 November 2006; accepted 16 November 2006

Available online 26 December 2006

Abstract

The breaking of the C–S bond in C_2H_5SH on the catalytically active (100) edge of 2H-MoS_2 was studied by means of density functional theory. Two reactions of C_2H_5SH were investigated: hydrogenolysis to ethane and elimination to ethane, with H_2S as second product in both cases. The adsorption geometry, involving a hydrogen atom of the methyl group of C_2H_5SH, conducted reactions to more strongly bound surface intermediate states. The C–S bond breaking resulting in ethane formation proceeds with a lower energy barrier than in ethene formation when the energy of the barriers for desorption of the products from the surface is compared relative to the molecularly adsorbed C_2H_5SH state.
© 2006 Elsevier Inc. All rights reserved.

Keywords: Density functional theory; Hydrodesulfurization; C–S bond breaking; Hydrogenolysis; Elimination; Sulfide catalysis; Molybdenum disulfide

1. Introduction

In the catalytic hydrodesulfurization (HDS) of crude oil, sulfur is removed from fuels such as naphtha or gas oil by passing the fuels at high hydrogen pressures over a catalyst to decompose organic sulfur-containing molecules to hydrocarbons and hydrogen sulfide. The most widely used catalysts contain MoS_2 phases promoted with cobalt or nickel [1,2]. Organosulfur compounds present in petroleum fractions differ in molecular size and structure and thus also in reactivity. Dibenzothiophene and 4,6-dialkyldibenzothiophene are difficult to desulfurize; consequently, experimental [1–5] as well as theoretical investigations [6–12] have concentrated on the hydrodesulfurization of these molecules.

Two types of reactions are relevant in the sulfur removal from dibenzothiophene and 4,6-dialkyldibenzothiophene: direct desulfurization and hydrogenation followed by sulfur removal. In direct desulfurization, dibenzothiophene reacts with H_2 to biphenyl and H_2S. In the hydrogenation reaction, one of the benzene rings of dibenzothiophene is hydrogenated, and the resulting hexahydrodibenzothiophene reacts to cyclohexylbenzene and H_2S.

Despite intensive research, the nature of the C–S bond breaking in direct desulfurization remains under discussion. It has been proposed that direct desulfurization occurs by a real hydrogenolysis reaction, in which C–S bonds are broken and C–H and S–H bonds are formed simultaneously. In the case of dibenzothiophene, biphenyl forms on reaction with hydrogen during a sojourn on the catalyst surface [1–4]. Thus, direct desulfurization would be similar to hydrogenolysis of hydrocarbons on metal surfaces. Another possibility involves hydrogenation of dibenzothiophene, followed by elimination of H_2S to give biphenyl [5]. It also has been proposed that a metal atom might be inserted into the C–S bond followed by hydrogenation, as has been observed in organometallic complexes of thiophene and benzothiophene [13,14]; however, this is unlikely in the heterogeneous reaction, because of the rigidity of the catalyst structure. Even in the case of the much simpler alkane thiols, the mechanism of the hydrogenolysis reaction of alkanethiols to alkanes over metal sulfide catalysts has not well been studied [15,16]. The poor accessibility of metal sulfides to surface science studies has hampered progress in understanding the reactions of thiols on their surfaces. Much more work has been done on investigating the interaction of alkanethiols with metal

* Corresponding author. Fax: +41 44 632 1162.
E-mail address: thomas.weber@chem.ethz.ch (Th. Weber).

0021-9517/$ – see front matter © 2006 Elsevier Inc. All rights reserved.
doi:10.1016/j.jcat.2006.11.023

surfaces [17–21]. Such surfaces can be readily characterized by spectroscopic techniques, making them ideal for surface science model studies.

Thiols that lack a β-carbon atom react by hydrogenolysis to an alkane and H_2S. Therefore, the simplest thiol, methanethiol, is perfectly suited for studying the S–H bond activation and, more importantly, the catalytic C–S bond scission. The measured activation energies for the desulfurization reactions of C_2H_5SH and CH_3SH over MoS_2 catalysts are of the same order, but slightly lower in the case of C_2H_5SH. Chemical bonds in these molecules are activated in the order of H–H > H–S > C–S ≈ C–H (C_2 compounds) > C–H (C_1 compounds) ≫ C–C [16]. The activation energy for the disappearance of ethanethiol is 18 kcal/mol; the activation energies for ethene and ethane formation were 24 and 23 kcal/mol, respectively. On molybdenum metal, surface science experiments showed that only three gaseous products were formed in the reaction of ethanethiol on the Mo(110) surface: H_2, ethane, and ethene [22]. There was no evidence for the evolution of any other hydrocarbon, such as methane, acetylene, or benzene, or for the formation of gaseous sulfur-containing products. Ethanethiol did not desorb. Temperature-programmed reaction spectroscopy results suggested that on Mo(110), molecularly adsorbed ethanethiol decomposes slowly, followed by fast desorption of ethane and ethene.

Thiolates have been proposed as intermediates in hydrodesulfurization reactions. Thus, understanding their reactivity is important in modeling product distributions. Methanethiol dissociates to methanethiolate on Ni(111) [23], Pt(111) [24], Mo(110) [25], W(211) [17], Cu(100) [26], and Fe(100) [27]. The C–S bond of the methanethiolate intermediate is subsequently cleaved, yielding methane and H_2 as gaseous products along with surface carbon and sulfur. DFT calculations of the adsorption configurations of methanethiol on Au(111) also favored the formation of strongly bound thiolates [28,29]. Decomposition of ethanethiol over cadmium sulfide gave 24% ethene and 45% hydrogen sulfide at 900 K, along with some free sulfur, hydrogen, and diethylsulfide [30]. Similar results were obtained with the sulfides of nickel, copper, cobalt, and iron. On reduced iron, however, the decomposition of ethanethiol at 500 K gave 63% ethane and 25% ethene [31].

Neither molybdenum nor tungsten sulfide catalysts showed any activity for the rupture of the C–C bond of ethanethiol below 600 K [16]. The conversion of adsorbed ethyl radicals to gaseous ethane was not particularly rapid but occurred more readily than the corresponding desorption of methyl radicals as methane from methanethiol. In contrast, on metals, ethanethiol decomposes to elemental carbon and sulfur and gaseous dihydrogen [22].

In previous work, we studied by means of DFT calculations the adsorption, dissociation, and reaction of methanethiol on the catalytically active Mo edge of MoS_2 as a function of sulfur coverage and presence of hydrogen and promoter atoms [32]. The majority of thiols have a β-hydrogen atom, however, and they undergo not only hydrogenolysis to alkanes, but also H_2S elimination to alkenes. Consequently, in the present work we extended our study of the mechanism of the C–S bond scission with DFT calculations of these two reaction pathways for the dissociation of ethanethiol on the (100) catalytically active surface of 2H-MoS_2. This will provide a better understanding of HDS reactions, which occur in more complex reactions of larger sulfur-containing molecules.

2. Computational details

The theoretical method that we used in the DFT calculations was the same as described before [32]. We used the DMol^3 code [33] with a double-numeric polarized basis set, a medium level of integration grid consisting of approximately 1000 grid points per atom, and performed effective core potential calculations. With these settings, we calculated the energy of the gas-phase desulfurization reaction of C_2H_5SH to $C_2H_6 + S$ with 59.78 kcal/mol (experimental value, 55.08 kcal/mol) and the hydrogenation reaction of $C_2H_4 + H_2$ to C_2H_6 with 33.5 kcal/mol (experimental value, 32.5 kcal/mol) [34]. A combination of the local density approximation to specify the exchange correlation local potential [35] and corrected in the high- and low-density expansions as proposed by Perdew and Wang [36] was used. The Brillouin zone integration was performed using a set of $2 \times 2 \times 1$ k points. We selected a (4×1) surface supercell of the 2H-MoS_2 crystal structure with a vacuum slab of 9 Å and a slab thickness of 12 Å. The (4×1) surface model consists of two MoS_2 sheets in the y direction, six planes of atoms in the z direction (three MoS_2 units), and four surface Mo atoms in the x direction (Fig. 1). The (100) MoS_2 surface exhibits two types of edges. On one edge, unsaturated molybdenum atoms are exposed (the so-called Mo edge); on the other edge, sulfur atoms are exposed (the S edge). The geometries of all atoms in the slabs were optimized, using the following geometry optimization convergence thresholds: 0.01 kcal/mol (energy change), 2.5 kcal/mol × Å (maximum force), and 0.005 Å (maximum displacement).

To calculate the minimum energy path between several reaction steps, we used the linear/quadratic synchronous transit (LST/QST) method [37] proposed by Halgren and Lipscomb [38] and implemented in the DMol^3 code [33]. The activation energy is determined by the highest maximum on the minimum

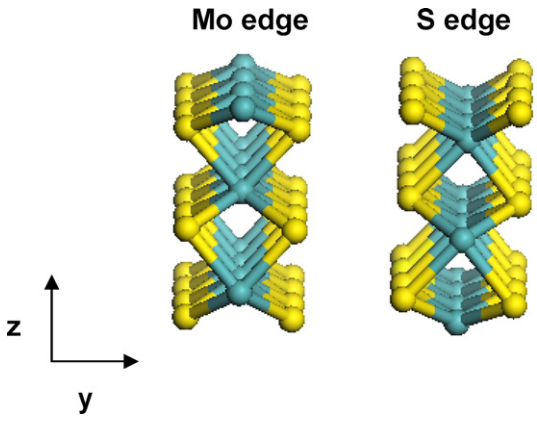

Fig. 1. (100) surface of 2H-MoS_2.

energy path, obtained by the LST/QST method. The reaction path connects the C_2H_5SH molecule above the surface, with the C_2H_4 or C_2H_6 molecule desorbed to the gas phase and the S atom bonded to the catalyst surface as final products. The path was divided into several steps between the reactant and products by interpolating along the path segments following the adiabatic valley of the potential surface. We calculated the energies of these steps, as well as the adsorption barriers. The success of the calculations with the LST/QST method is based on the close proximity of the endpoints for the transition state search. The transition state has been refined by optimizing the transition state following the eigenvector of the Hessian matrix corresponding to the imaginary frequency mode; thus, it has been verified that the transition states have only one imaginary frequency.

3. Results

Our study of the hydrogenolysis of CH_3SH showed that starting from the "as-cleaved" Mo edge of the MoS_2 surface, the formation of CH_4 from the adsorbed CH_3 fragment and the S–H group had a high activation barrier of 68.6 kcal/mol, due to the strong Mo–C and MoS–H bonds [32]. This high-energy barrier is due to the low coordination number of the surface molybdenum atoms relative to the bulk coordination number, and the tendency of the surface molybdenum atoms to compensate for this by adjusting the adsorbed species for optimal Mo–S and Mo–C interactions. The energy barrier decreased when sulfur atoms were present on the Mo edge in bridging positions between the Mo atoms, and the lowest barrier was obtained for a surface with one sulfur atom less than the maximal possible coverage (i.e., a surface with one sulfur vacancy). Combined thermodynamic and DFT calculations have shown that the Mo edge of the MoS_2 crystallites is strongly covered with sulfur atoms under HDS reaction conditions ($0.01 < H_2S/H_2 < 0.1$) [6–10,12]. To allow adsorption of the thiol molecule, the $(10\bar{1}0)$ Mo edge should not be completely covered with sulfur. Therefore, we performed three types of calculations on reactions of C_2H_5SH on MoS_2 surfaces, where the Mo edge is covered with sulfur atoms by 25, 50, or 75%. These situations are implemented in the calculations by adsorbing one, two, or three sulfur atoms on the (4×1) surface supercell (Fig. 1). In the classical way of thinking, these states correspond to three sulfur vacancies, two sulfur vacancies, and one sulfur vacancy, respectively. In agreement with others [6–10], our calculations showed that the most stable positions for the sulfur atoms are in bridging positions between Mo atoms. Therefore, in the first calculation the Mo edge contains two four-coordinated and two five-coordinated Mo atoms, in the second calculation it contains four five-coordinated Mo atoms, and in the third calculation it contains two five-coordinated and two six-coordinated Mo atoms. The latter configuration resembles the (100) MoS_2 catalyst surface when a vacancy has been created, similar to what has been demonstrated by scanning tunneling microscopy [39,40].

3.1. 25% sulfur coverage

In the first series of calculations, a C_2H_5SH molecule was positioned at a distance $z = 4.5$ Å above a Mo-terminated surface containing one adsorbed sulfur atom. Subsequently C_2H_5SH was molecularly adsorbed on this sulfided surface. In the most stable state, a hydrogen atom from the CH_3 group had a distance of only 2.1 Å to the surface sulfur atom, that is, $d(S_{surf}–H_{methyl}) = 2.1$ Å. Fig. 2 shows the reaction path for

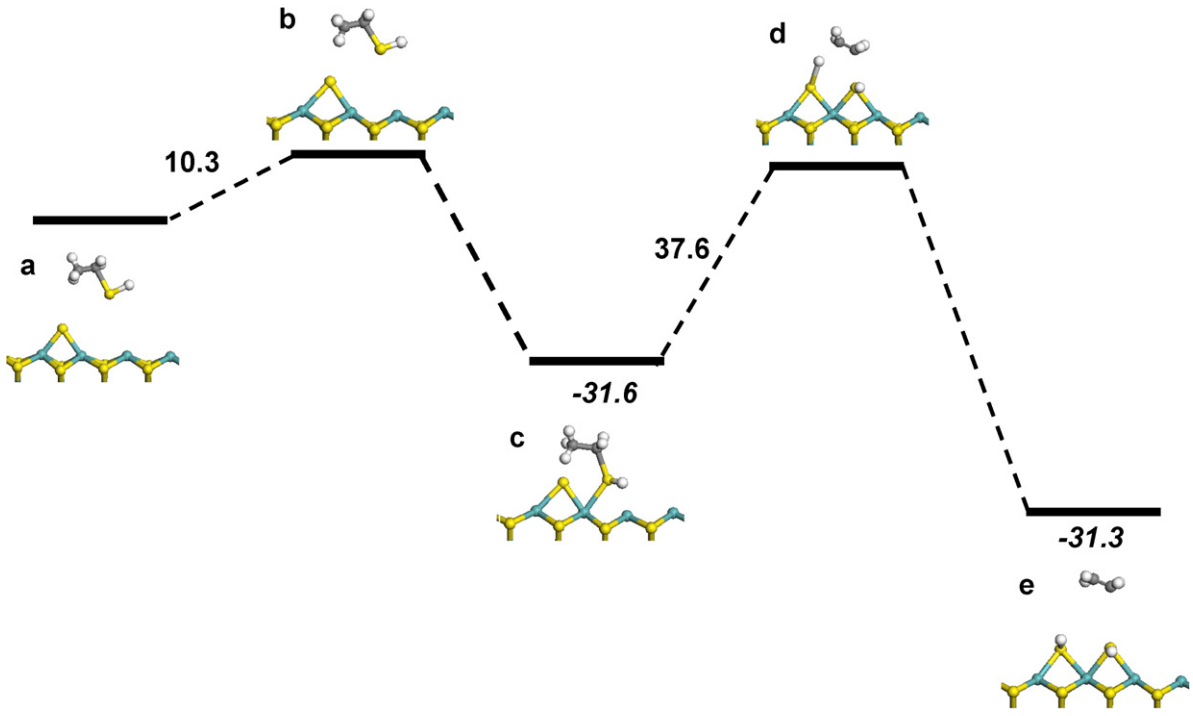

Fig. 2. Elimination, resulting in ethene formation from molecularly adsorbed C_2H_5SH on a surface with three sulfur vacancies.

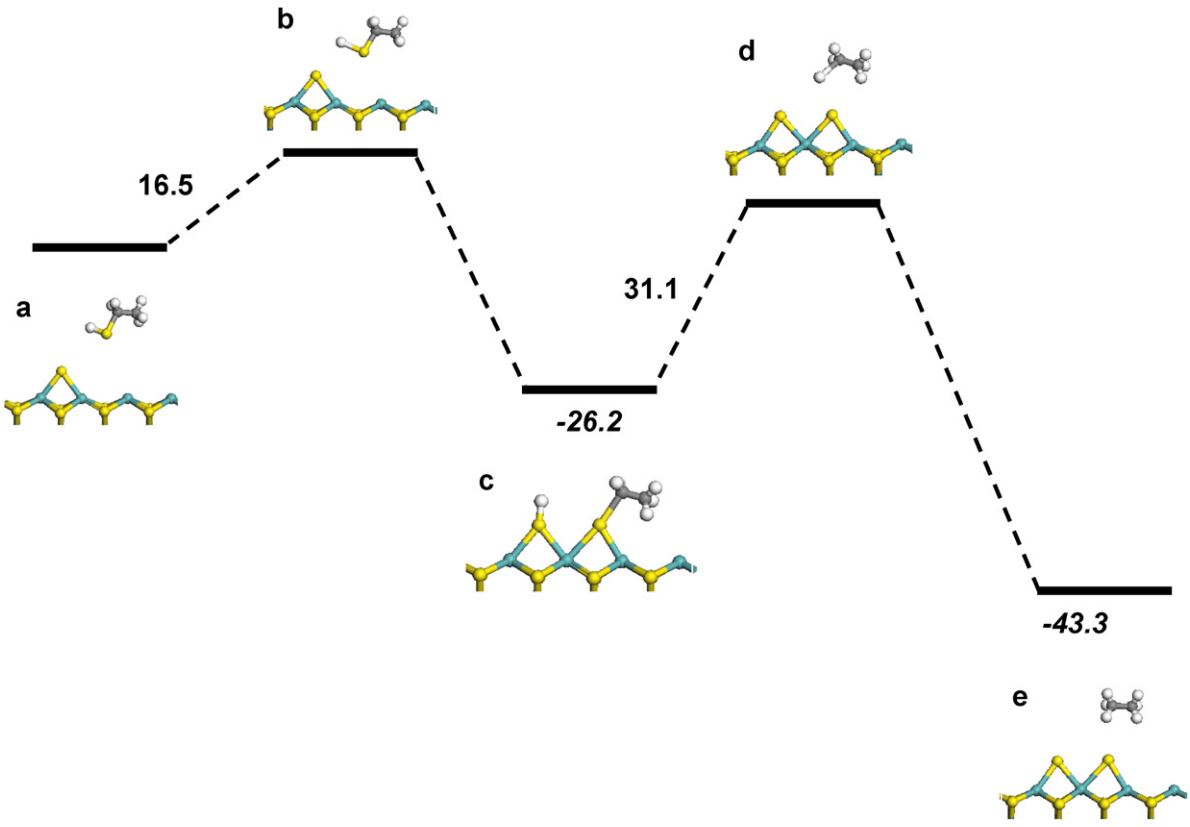

Fig. 3. Hydrogenolysis, resulting in ethane formation from adsorbed C_2H_5S and H fragments on a surface with three sulfur vacancies.

molecular C_2H_5SH adsorption, followed by H_2S elimination, which results in the formation of C_2H_4 and two surface SH species in bridging positions. The energy of the reaction from the initial state (with the C_2H_5SH molecule 4.5 Å above the surface; Fig. 2a) to the intermediate state (molecularly adsorbed C_2H_5SH; Fig. 2c) was −31.6 kcal/mol, whereas the energy barrier was 10.3 kcal/mol (Fig. 2, a → b).

Compared with CH_3SH, for which dissociative adsorption occurred (i.e., formation of CH_3S and H fragments [$\Delta E = -38.9$ kcal/mol]), the molecular adsorption of C_2H_5SH led to a less stable intermediate state ($\Delta E = -31.6$ kcal/mol; Fig. 2c). Both thiols showed a clear tendency for bonding in bridging arrangements. The adsorption geometry of the SH species reflects the preference of the sulfur atom for high coordination to the Mo atoms, whereas the hydrogen atom adsorbs out of the surface plane due to repulsion [41]. The desorption barrier of C_2H_4 was calculated with 37.6 kcal/mol (Fig. 2, c → d), whereas in the hydrogenolysis of CH_3SH, the formation of CH_4 had an activation barrier of 46.0 kcal/mol [32]. The transition state (Fig. 2d) involves a deformed, nonplanar ethene with weak interactions to the surface sulfur atom via a weakly bonded hydrogen atom. The final state (Fig. 2e) consists of two S–H groups in bridging positions between two Mo atoms and a C_2H_4 molecule in the gas phase. It is 31.3 kcal/mol lower in energy than the intermediate molecular adsorption state (Fig. 2c). Thus, the overall exothermicity of this process is 62.9 kcal/mol.

Along with elimination, ethanethiol can also undergo hydrogenolysis, resulting in ethane formation from the adsorbed C_2H_5S and H fragments. In the initial state, the distance between the sulfur atom of the surface and the hydrogen atom of the C_2H_5SH molecule was $z = 2.8$ Å (Fig. 3a). The reaction energy of an C_2H_5SH molecule above the MoS_2 surface to adsorbed C_2H_5S and H fragments was −26.2 kcal/mol (Fig. 3, a → c) with an energy barrier of 16.5 kcal/mol (Fig. 3, a → b). The experimental activation energy associated with the dissociation of ethanethiol on MoS_2 was reported to be 18 kcal/mol [16]. This energy barrier is higher than that reported for dissociation on the metallic Mo(110) surface, <7 kcal/mol [42], because the M–S bonding on the surface of a transition-metal sulfide is weaker than on the surface of the metal. The energy barrier for the second step (i.e., C_2H_6 formation) was 31.1 kcal/mol (Fig. 3, c → d). The final state, consisting of a C_2H_6 molecule in the gas phase above the Mo-terminated surface of the (4 × 1) supercell containing two sulfur atoms in bridging positions (Fig. 3e), was energetically 43.3 kcal/mol lower than the intermediate state (Fig. 3c), and the overall process was exothermic by 69.5 kcal/mol.

In the case of CH_3SH, the formation of CH_4 via hydrogenolysis is exothermic by 68.5 kcal/mol [32]. This slight energy difference is in good agreement with thermochemical data, which predict the hydrogenolysis reaction of CH_3SH to be slightly more exothermic by 3.3 kcal/mol.

3.2. 50% sulfur coverage

In the second series of calculations, we adsorbed a C_2H_5SH molecule on an Mo edge with two surface sulfur atoms in bridging positions on the (4 × 1) surface supercell. This ini-

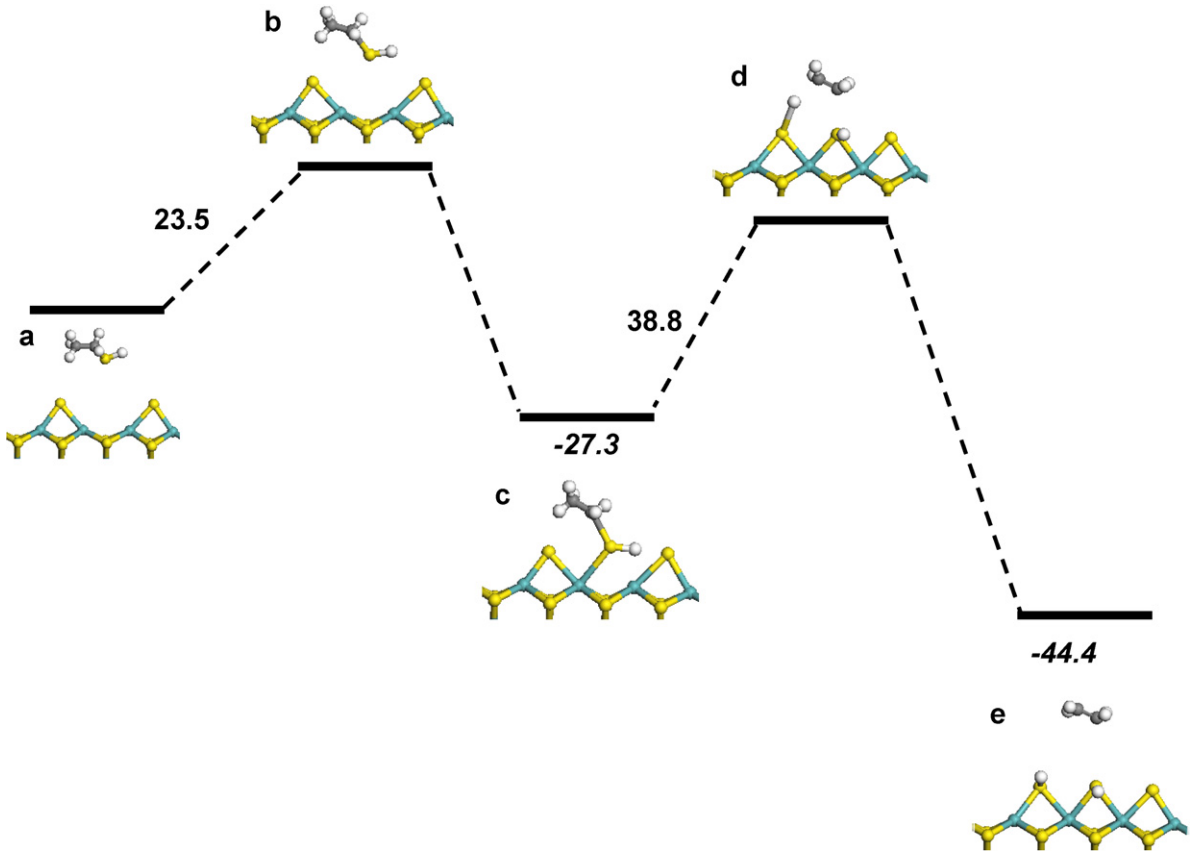

Fig. 4. Elimination, resulting in ethene formation from molecularly adsorbed C_2H_5SH on a surface with two sulfur vacancies.

tial state was similar to that of the previously discussed case; a hydrogen atom of the methyl group of ethanethiol gets rather close to a surface sulfur atom with $d(S_{surf}–H_{methyl}) = 2.2$ Å (Fig. 4c). The energy barrier for this adsorption configuration is higher (23.5 kcal/mol; Fig. 4, a → b) than for adsorption on a Mo edge covered with only one S atom (10.3 kcal/mol; Fig. 2, a → b). Furthermore, the intermediate state is less stable, −27.3 kcal/mol (Fig. 4c), compared with −31.6 kcal/mol (Fig. 2c). The formation of C_2H_4 had an activation energy of 38.8 kcal/mol (Fig. 4, c → d). The final state has two S–H groups and one sulfur atom in a bridging mode between two molybdenum atoms on the surface (Fig. 4e) and is 44.4 kcal/mol more stable than the intermediate state.

The C_2H_5SH molecule also can react by hydrogenolysis (i.e., ethane formation), starting from the intermediate indicated in Fig. 4c. The energy barrier for ethane formation was 28.0 kcal/mol (Fig. 5, c → d), and the C_2H_6 molecule was stretched in the transition state (Fig. 5d). The final state (Fig. 5e), with a highly sulfided surface (formal degree of sulfidation, 75%) and a C_2H_6 molecule in the gas phase, was 36.2 kcal/mol more stable than the intermediate state (Fig. 5c), which represents the molecular adsorption of C_2H_5SH. Because of the larger size of the C_2H_5SH molecule compared with CH_3SH, the energy for adsorption on the surface was higher and the transition state (Fig. 5b) different than the respective transition state in the reaction of CH_3SH [32]. Whereas molecular dissociation and adsorption are easy for the smaller CH_3SH, this is not the case for C_2H_5SH. However, once on the surface, the energy barriers for desorption of the hydrogenolysis products were similar, 30.0 kcal/mol for CH_4 formation and 28.0 kcal/mol for C_2H_6 formation.

3.3. 75% sulfur coverage

In the third series of calculations, a C_2H_5SH molecule was adsorbed on the Mo edge with three sulfur atoms on the (4×1) surface supercell, exposing two five-coordinated and two six-coordinated molybdenum atoms (Fig. 6). The results were similar to those of the foregoing calculation. In the intermediate state (Fig. 6c), the C_2H_5SH molecule adsorbed on the sulfur vacancy, and the H atom occupied a position out of the Mo plane. The activation energy barrier was 24.6 kcal/mol (Fig. 6, a → b), and the reaction energy was −25.9 kcal/mol (Fig. 6, a → c). The formation of C_2H_4 had an activation energy of 36.7 kcal/mol (Fig. 6, c → d). The final state had two S–H groups and two sulfur atoms in a bridging mode between two molybdenum atoms on the surface (Fig. 6e) and was 48.1 kcal/mol more stable than the intermediate state.

The second step of the hydrogenolysis reaction, i.e., the formation of C_2H_6 from the adsorbed C_2H_5SH molecule and its release from the surface had a barrier of 25.6 kcal/mol (Fig. 7, c → d) and a reaction energy of −46.4 kcal/mol (Fig. 7, c → e). This second activation energy was even lower than that for the surface with two S atoms (Fig. 5) and confirms the positive influence of S atoms on the Mo-terminated edge. All calculated energy values are compiled in Table 1.

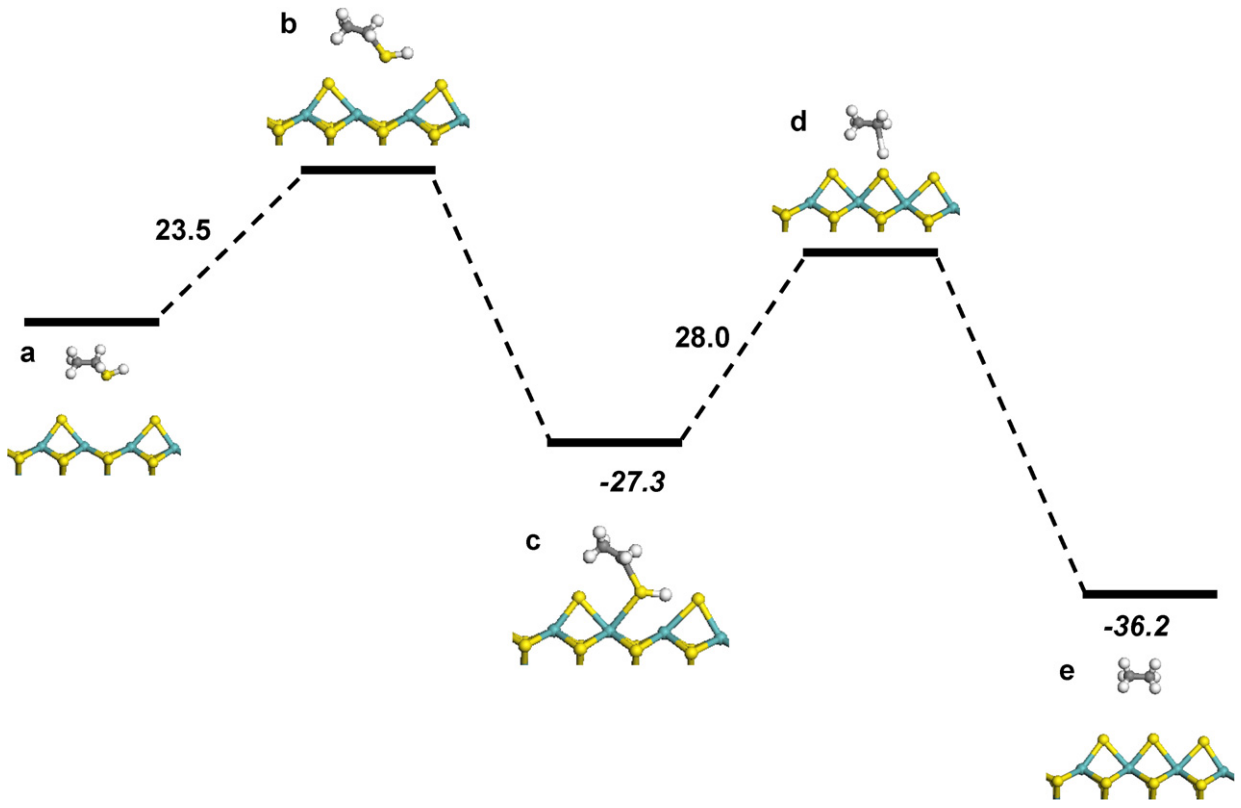

Fig. 5. Hydrogenolysis, resulting in ethane formation from molecularly adsorbed C_2H_5SH on a surface with two sulfur vacancies.

Table 1
Activation energies and energy differences (in kcal/mol) in the reactions of C_2H_5SH to H_2S and C_2H_4 or C_2H_6 as functions of the number (N) of bridging S atoms on the Mo edge

Edge	N	C_2H_4				C_2H_6			
		$E_a(1)$	$-\Delta E(1)$	$E_a(2)$	$-\Delta E(2)$	$E_a(1)$	$-\Delta E(1)$	$E_a(2)$	$-\Delta E(2)$
Mo	1	10.3	31.6	37.6	31.3	16.5	26.2	31.1	43.3
	2	23.5	27.3	38.8	44.4	23.5	27.3	28.0	36.2
	3	24.6	25.9	36.7	48.1	24.6	25.9	25.6	46.4

4. Discussion

Theoretical modeling suggested that metal–sulfur bonding plays an essential role in the desulfurization process of sulfur-containing molecules on various metal–sulfide catalysts [43]. Our results show that the C–S bond in the adsorbed thiolate is slightly longer and consequently weaker than in the thiol, and that the C–S bond scission and C–H bond formation occur nearly simultaneously.

The molybdenum atoms of the $(10\bar{1}0)$ Mo edge have a lower metal coordination number, a smaller d bandwidth, and hence a higher energy of the d band center than the corresponding bulk atoms [41,44]. The lower the coordination number of the surface metal atom is, the higher its reactivity. Sulfur adsorption on the $(10\bar{1}0)$ Mo edge increases the metal coordination number. Furthermore, the interaction between the occupied sulfur lone pairs of C_2H_5SH and the empty $4d$ orbitals of the molybdenum atom lowers the energy of the d band and stabilizes the thiolates on the surface.

Our calculations indicate low energy barriers for dissociation when the molecule is positioned initially close to a surface kink, resulting in a distance between the surface sulfur atom and the hydrogen atom of ethanethiol of 2.8 Å (Fig. 3). Molecular adsorption (10.3 kcal/mol; Fig. 2) and dissociation (16.5 kcal/mol; Fig. 3) on surfaces exposing metal atoms are easy steps, whereas the desorption of the final products ethene (37.6 kcal/mol; Fig. 2) and ethane (31.1 kcal/mol; Fig. 3) are less easy. Molecular adsorption at a sulfur vacancy of a sulfided surface has a higher adsorption barrier (23.5 kcal/mol; Figs. 4 and 5). At the same time, the energy barrier for the ethane formation is reduced to 28.0 kcal/mol (Fig. 5), and the energy for the ethene formation (38.8 kcal/mol) differed by only 1.2 kcal/mol from that of the elimination on a surface with one sulfur atom (Figs. 2 and 4). Therefore, the energy barriers for C_2H_6 formation and desorption from C_2H_5SH are dependent on the surface sulfur coverage, as in the case of CH_4 formation and desorption from CH_3SH [32]. Comparing the energy barriers for the C_2H_4 formation and desorption (Figs. 2, 4, and 6), our results do not show a clear dependence on the surface sulfur coverage, as far as the three investigated cases are concerned.

What are now the implications for hydrotreating catalysis? We showed in our previous work that the dissociation of CH_3SH on different edge surfaces of MoS_2 occurs on a pair of sulfur–metal sites under formation of SH groups and CH_3S species that are adsorbed in bridging positions between two surface metal atoms. In a second step, the hydrogen atom of the SH group moves to the neighboring CH_3S species to form CH_4.

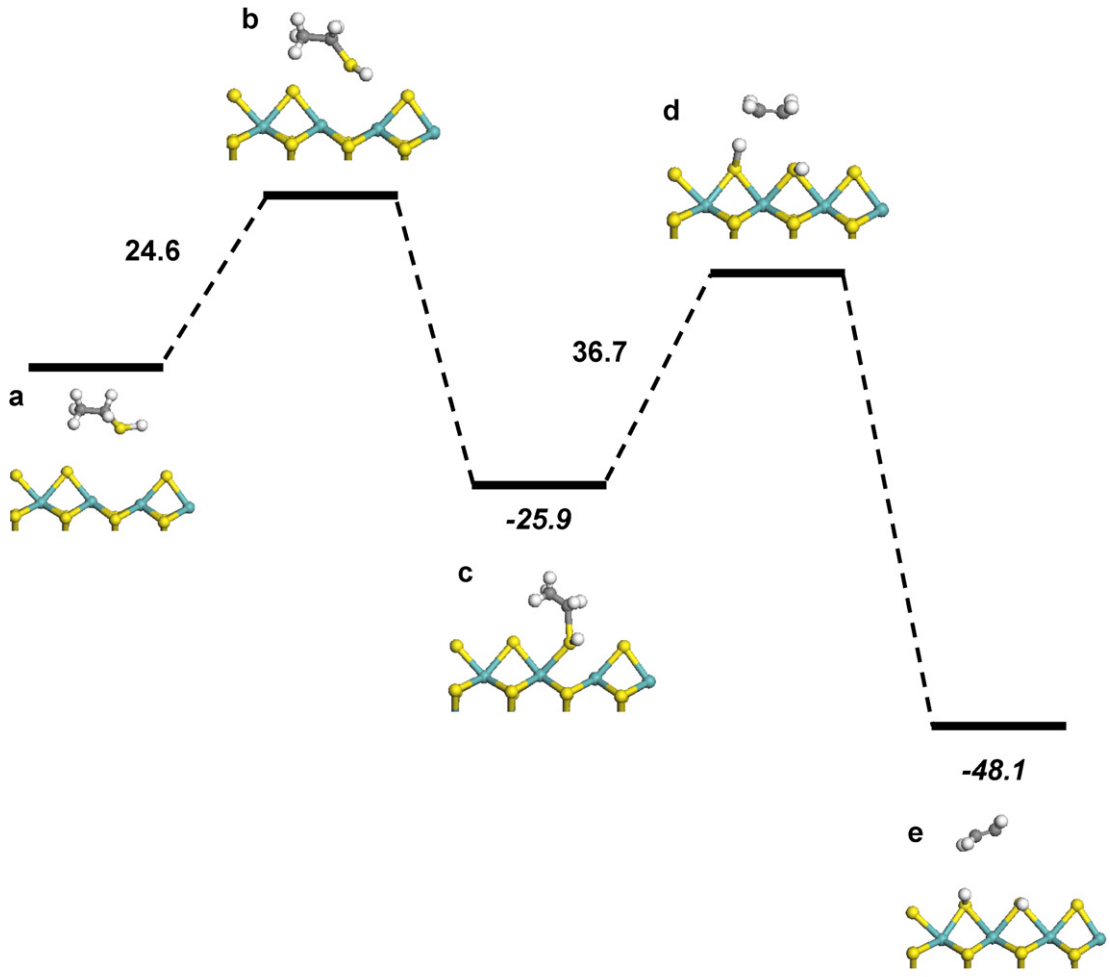

Fig. 6. Elimination, resulting in ethene formation from molecularly adsorbed C_2H_5SH on a surface with one sulfur vacancy.

The mechanism is identical to that proposed for the dissociation of H_2. However, the difference in geometric structures and chemical properties of these sulfur–metal pairs is clearly affected by the number of sulfur atoms on the metal surfaces. Consequently, different energy barriers for adsorption and desorption processes have been calculated, leading to different kinetic behaviors. Metal edge structures that are completely covered with sulfur atoms require an associative rather than a dissociative adsorption mechanism.

In this respect, our calculations show that the decomposition of ethanethiol to ethane and ethene are easy reactions. The energy diagrams (Figs. 2 and 3) indicate that also the reverse reactions will be relatively easy. This means that the hydrogenation reaction of a double bond very well could occur on the fully sulfided Mo edge and does not require a vacancy. As we have seen in the foregoing, the forward decomposition reactions of ethanethiol are

$$C_2H_5SH + * + S^* \rightarrow C_2H_5S^* + H\text{–}S^* \rightarrow C_2H_6 + 2S^* \quad (1)$$

and

$$\rightarrow C_2H_4 + 2H\text{–}S^*. \quad (2)$$

This opens a pathway for the formation of ethane from ethene via the following sequence of reactions (the reverse of the reactions shown in Figs. 2 and 3):

$$C_2H_4 + 2H\text{–}S^* \rightarrow C_2H_5S^* + H\text{–}S^* \rightarrow C_2H_6 + 2S^*. \quad (3)$$

The hydrogen atoms needed for the hydrogenation step might come from neighboring SH groups, which can be formed by dissociative adsorption of H_2 on the fully sulfided metal edge, as discussed previously [32], according to

$$H_2 + 2S^* \rightarrow 2H\text{–}S^*. \quad (4)$$

Such surface species can react further, as discussed previously [32], according to

$$2H\text{–}S^* \rightleftarrows H_2S + * + S^*. \quad (5)$$

Reaction (3) explains why Kieran and Kemball [16] observed that the exchange rate of an H atom of the ethyl group of ethanethiol with deuterium is similar to that of the exchange of ethene with deuterium, because in both cases a surface ethanethiolate intermediate is involved. Reaction (3) would also explain the "bean-like" structures observed by Lauritsen et al. in the STM pictures of the edges of triangular MoS_2 nanoclusters after treatment with hydrogen atoms and exposure to thiophene at 500 K [45]. They suggested that adsorbed

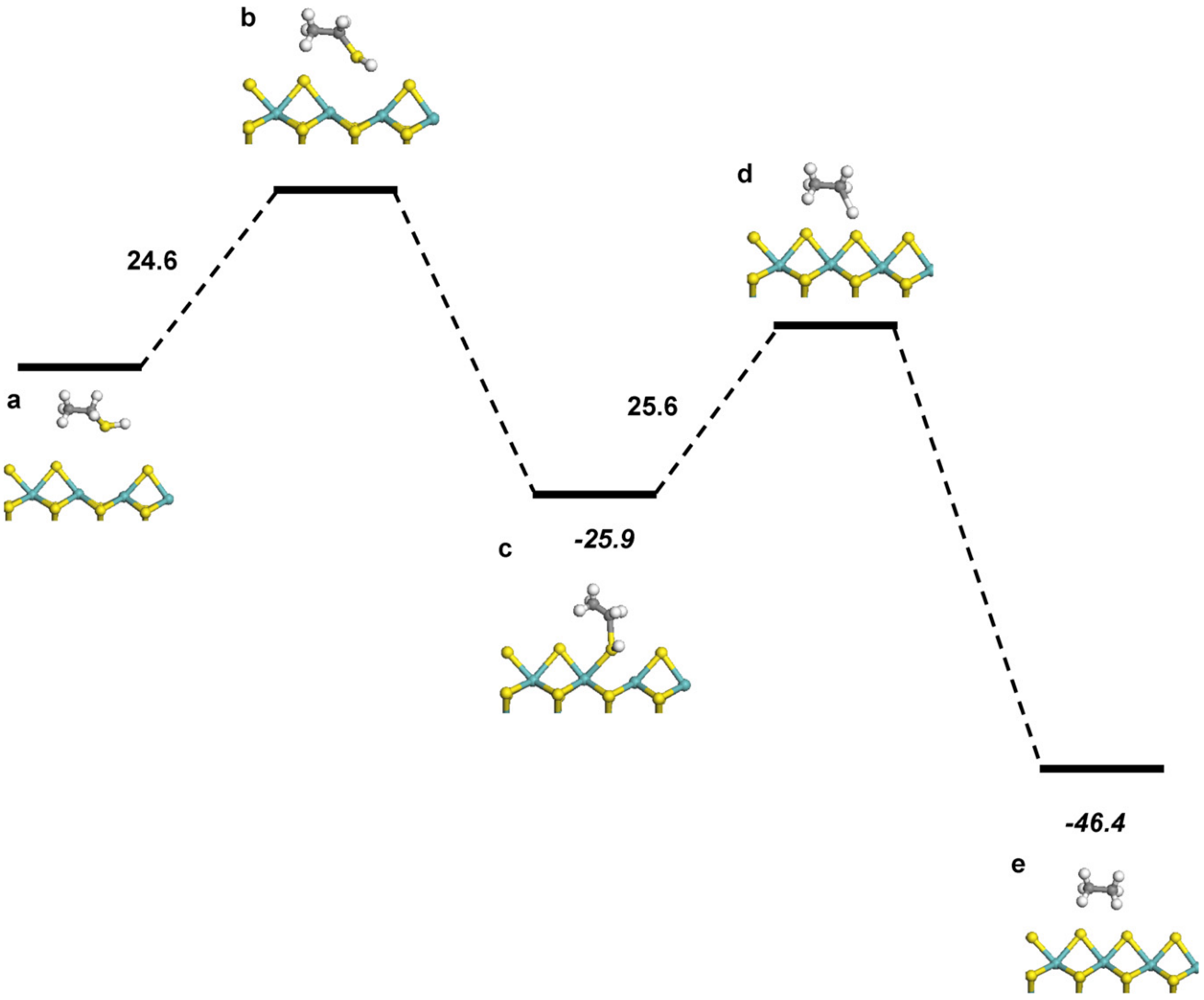

Fig. 7. Hydrogenolysis, resulting in ethane formation from molecularly adsorbed C_2H_5SH on a surface with one sulfur vacancy.

H atoms hydrogenate the thiophene at the fully sulfided MoS_2 edge to 2,5-dihydrothiophene, which then further reacts to but-2-enethiolate. The latter fragment would be the origin of the observed "bean-like" structure. Their DFT calculations indicated that the final C–S bond cleavage would require a modest activation energy of about 23 kcal/mol, but they did not calculate the barrier for the hydrogenation step. Of course, in the HDS of thiophene, not all reaction steps can occur on a fully sulfided Mo edge. In the final C–S bond-breaking step, the S atom needs a place to adsorb at the catalyst surface. On the other hand, borrowing from organometal chemistry, one could suggest that an associative, rather than a dissociative mechanism at the catalyst surface might explain why no vacancy is needed if H–S* groups are present on the catalyst's surface:

$$RSH + H\text{–}S^* \rightarrow R\text{–}S^* + H_2S. \quad (6)$$

Lauritsen et al. proposed another reaction that would not need a surface vacancy, namely that the but-2-enethiolate becomes bonded to a surface sulfur atom, apparently forming an alkyldisulfide fragment (R–S–S),

$$RSH + 2S^* \rightarrow R\text{–}S\text{–}S^* + H\text{–}S^*. \quad (7)$$

They assumed that the final sulfur extrusion must occur at a vacancy, however.

5. Conclusion

After molecular adsorption or decomposition on the (100) MoS_2 surface C_2H_5SH showed slightly lower energy barriers for desorption of the reaction products than CH_3SH. The C_2H_6 formation and desorption from ethanethiolate proceeded with a lower energy barrier than the C_2H_4 formation and desorption from the molecularly adsorbed C_2H_5SH state. The adsorption geometry, involving a hydrogen atom from the methyl group of C_2H_5SH, conducted reactions to more strongly bound intermediates. Whereas the energy barriers for C_2H_6 desorption from the surface are dependent on the surface sulfur coverage, as in the case of CH_4 formation starting from CH_3SH, the reaction

paths investigated for C_2H_4 formation showed similar energy barriers for desorption from surfaces with one, two, and three sulfur atoms.

The geometry of the adsorbed sulfur-containing molecule at the (10$\bar{1}$0) Mo edge is very important for analyzing the product distribution. Molecules with one carbon atom split into H and CH_3S fragments and adsorb on the surface. Larger molecules, like C_2H_5SH, also show a tendency for molecular adsorption.

Acknowledgments

This work was supported by Shell Global Solutions International BV. The authors thank Drs. V. Alexiev (Sofia) and J.A.R. van Veen (Amsterdam, Eindhoven) for valuable discussions.

References

[1] R. Prins, V.H.J. de Beer, G.A. Somorjai, Catal. Rev. Sci. Eng. 31 (1989) 1.
[2] H. Topsøe, B.S. Clausen, F.E. Massoth, Hydrotreating Catalysis, Science and Technology, Springer, Berlin, 1996.
[3] M.J. Girgis, B.C. Gates, Ind. Eng. Chem. Res. 30 (1991) 2021.
[4] D.D. Whitehurst, T. Isoda, I. Mochida, Adv. Catal. 42 (1998) 345.
[5] F. Bataile, J.L. Lemberton, P. Michaud, G. Pérot, M. Vrinat, M. Lemaire, E. Schulz, M. Breysse, S. Kasztelan, J. Catal. 191 (2000) 409.
[6] P. Raybaud, J. Hafner, G. Kresse, S. Kasztelan, H. Toulhoat, J. Catal. 189 (2000) 129.
[7] P. Raybaud, J. Hafner, G. Kresse, S. Kasztelan, H. Toulhoat, J. Catal. 190 (2000) 128.
[8] M. Sun, A.E. Nelson, J. Adjaye, J. Catal. 226 (2004) 32.
[9] S. Cristol, J.F. Paul, E. Payen, D. Bougeard, S. Clemendot, F. Hutschka, J. Phys. Chem. B 104 (2000) 11220.
[10] S. Cristol, J.F. Paul, E. Payen, D. Bougeard, S. Clemendot, F. Hutschka, J. Phys. Chem. B 106 (2002) 5659.
[11] A. Travert, H. Nakamura, R.A. van Santen, S. Cristol, J.F. Paul, E. Payen, J. Am. Chem. Soc. 124 (2002) 7084.
[12] S. Cristol, J.F. Paul, E. Payen, D. Bougeard, F. Hutschka, S. Clemendot, J. Catal. 224 (2004) 138.
[13] R.J. Angelici, in: Th. Weber, R. Prins, R.A. van Santen (Eds.), Transition Metal Sulfides, Chemistry and Catalysis, Kluwer Academic, Dordrecht, 1998, p. 89.
[14] C. Bianchini, A. Meli, in: Th. Weber, R. Prins, R.A. van Santen (Eds.), Transition Metal Sulfides, Chemistry and Catalysis, Kluwer Academic, Dordrecht, 1998, p. 129.
[15] R.L. Wilson, C. Kemball, J. Catal. 3 (1964) 426.
[16] P. Kieran, C. Kemball, J. Catal. 4 (1965) 380.
[17] J.B. Benziger, R.E. Preston, J. Phys. Chem. 89 (1985) 5002.
[18] C.M. Friend, J.T. Roberts, Acc. Chem. Res. 21 (1988) 394.
[19] D.R. Huntley, J. Phys. Chem. 93 (1989) 6156.
[20] B.C. Wiegand, C.M. Friend, Chem. Rev. 92 (1992) 491.
[21] S.M. Kane, T.S. Rufael, J.L. Gland, D.R. Huntley, D.A. Fischer, J. Phys. Chem. B 101 (1997) 8486.
[22] J.T. Roberts, C.M. Friend, J. Chem. Phys. 92 (1988) 5205.
[23] T.S. Rufael, D.R. Huntley, D.R. Mullins, J.L. Gland, J. Phys. Chem. 99 (1995) 11472.
[24] T.S. Rufael, J. Prasad, D.A. Fischer, J.L. Gland, Surf. Sci. 278 (1992) 41.
[25] B.C. Wiegand, P. Uvdal, C.M. Friend, Surf. Sci. 279 (1992) 105.
[26] B.A. Sexton, G.L. Nyberg, Surf. Sci. 165 (1986) 251.
[27] M.R. Albert, J.P. Lu, S.L. Bernasek, S.D. Cameron, J.L. Gland, Surf. Sci. 206 (1988) 348.
[28] H. Grönbeck, A. Curioni, W. Andreoni, J. Am. Chem. Soc. 122 (2000) 3839.
[29] M. Konopka, R. Rousseau, I. Stich, D. Marx, J. Am. Chem. Soc. 126 (2004) 12103.
[30] J.L. Boivin, R. Macdonald, Can. J. Chem. 33 (1955) 1281.
[31] A.N. Bushkirov, N.L. Barabanov, Dokl. Akad. Nauk SSSR 104 (1955) 854.
[32] T. Todorova, R. Prins, Th. Weber, J. Catal. 236 (2005) 190.
[33] B. Delley, J. Chem. Phys. 92 (1990) 508;
B. Delley, J. Chem. Phys. 113 (2000) 7756.
[34] A. Maiti, N. Govind, P. Kung, D. King-Smith, J.E. Miller, C. Zhang, G. Whitwell, J. Chem. Phys. 117 (2002) 8080.
[35] S.H. Vosko, L. Wilk, M. Nusair, Can. J. Phys. 58 (1980) 1200.
[36] J.P. Perdew, Y. Wang, Phys. Rev. B 45 (1992) 13244.
[37] N. Govind, M. Petersen, G. Fitzgerald, D. King-Smith, J. Andzelm, Comput. Mat. Sci. 28 (2003) 250.
[38] T.A. Halgren, W.N. Lipscomb, Chem. Phys. Lett. 49 (1977) 225.
[39] S. Helveg, J.V. Lauritsen, E. Lægsgaard, I. Stensgaard, J.K. Nørskov, B.S. Clausen, H. Topsøe, F. Besenbacher, Phys. Rev. Lett. 84 (2000) 951.
[40] J.V. Lauritsen, M.V. Bollinger, E. Lægsgaard, K.W. Jacobsen, J.K. Nørskov, B.S. Clausen, H. Topsøe, F. Besenbacher, J. Catal. 221 (2004) 510.
[41] B. Hammer, J.K. Nørskov, Adv. Catal. 45 (2000) 71.
[42] C.M. Friend, J.T. Roberts, Acc. Chem. Res. 21 (1988) 394.
[43] T.A. Pecoraro, R.R. Chianelli, J. Catal. 67 (1981) 430.
[44] V. Alexiev, R. Prins, Th. Weber, Phys. Chem. Chem. Phys. 3 (2001) 5326.
[45] J.V. Lauritsen, M. Nyberg, R.T. Vang, M.V. Bollinger, B.S. Clausen, H. Topsøe, K.W. Jacobsen, E. Lægsgaard, J.K. Nørskov, F. Besenbacher, Nanotechnol. 14 (2003) 385.